

PROJECT REPORT

REPORT NUMBER: GBM-120816-1-RP1

DATE: April 11, 2017

CLIENT INFORMATION

GBMc and Associates
219 Brown Lane
Bryant, AR 72022
Attn: Chuck Campbell

SAMPLE DISCRPTION

One crate containing two (2) pipe samples was received by motor freight (FedEx Freight Bill 3866606645) on December 1, 2016. Each sample was approximately 91 inches in overall length and contained a gasketed bell and spigot joint in the approximate middle of the sample. The samples were labeled "E1" and "E2" and contained witness signature of "Chuck Campbell." Figure 1 below displays one of the samples during the uncrating process.



Figure 1. Digital image of one sample during uncrating.

Figures 2 and 3 display the joint areas of the individual samples and associated witness marks. The bell section of Sample E1 was 52 inches in length and the bell section of Sample E2 was 55 inches in length. The spigot lengths (from the bell lip) were 39 inches and 36 inches, respectively, for Sample E1 and Sample E2. Because the joints were not water tight (and pressure testing could not be performed on the samples as-received) the pipe barrel sections of the samples were shortened by approximately 2-3 feet on each side of the joint to facilitate handling.

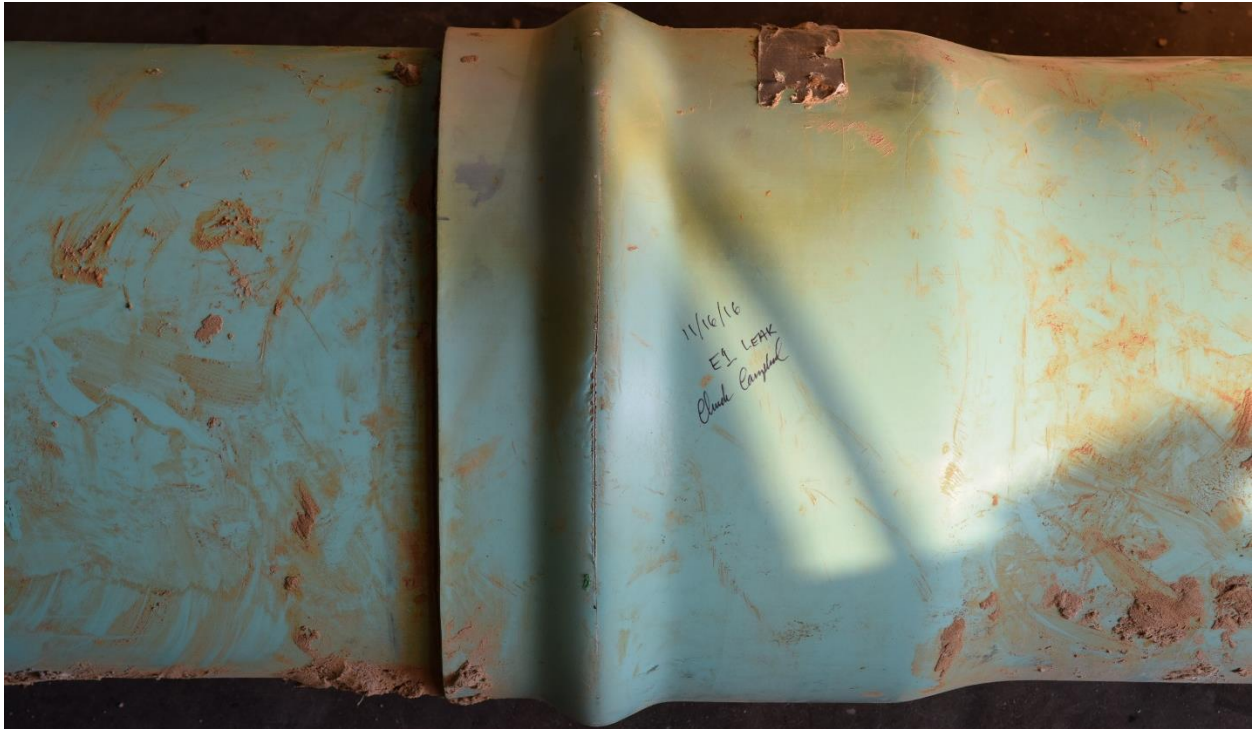


Figure 2. Digital image of Sample E1 with removal date of 11/16/16.



Figure 3. Digital image of Sample E2 with removal date of 11/15/16.

The bell printline of Sample E1 reads:
...905 JM80 AD 2012/MAR/27 06:01 TREATED WASTEWATER...

The spigot printline of Sample E1 is practically identical, except for MARCH 25 production date code.

The composite printline of Sample E2 reads:
...14" CI PVC1120 DR32.5 125 PSI T250 AWWA C905 JM80 AD 2012/MAR/25 17:46
TREATED WASTEWATER JM EAGLE U.S. GREEN BUILDING COUNCIL MEMBER...

The client reported:

1. The pipeline is an approximately 12,500 foot long section of 14-inch nominal diameter in DR32.5 (AWWA C905 Pressure Class 125 psi) and DR25 (AWWA C905 Pressure Class 165 psi).
2. The pipe was all manufactured by JM Eagle and was purchased as a single lot by the pipeline group and stored locally until installed (March 2012 date code).
3. The pipeline was installed in 2013 and became operation in approximately September of 2013.
4. The pipeline operates as a treated wastewater force main with typical operating pressure (during pumping) of 75 psi.
5. All failures have been in the DR32.5 portion of the pipeline.
6. There have been seventeen (17) total failures to date (as of April 7, 2017).
7. The first failure was discovered in October 2016.
8. The early failures exhibited circumferential bell fractures at the crown of the gasket race.
9. The circumferential fractures have generally been located in the upper half of the pipe, or the as-installed 12 o'clock position.
10. A second failure mode was identified within excavated samples observed during a site visit by S. Ferry the week of March 13, 2017 consisting of joint leakage without visible fracture.
11. Within the seventeen total failures, thirteen (13) display the circumferential bell failure mode, and four (4) display the joint leakage failure mode.
12. The failures have all occurred within approximately the first 5350 feet of the pipeline just downstream of the discharge point from the chemical manufacturing facility.
13. The first failure is approximately 150 feet from the GLCC pump station into the line.
14. The pipeline was designed to be fully filled at all times, although with intermittent cyclic flow.
15. Flow velocities were designed to be <5 fps.

TESTS PERFORMED and RESULTS

A comprehensive array of inspections and tests were brought to bear in order to gain an understanding of the overall failure mode and confirm or refute various potential causes of failures.

The samples were inspected upon receipt and found to be appropriately belled (i.e. the spigots were inserted to the manufacturer's minimum insertion mark). Note that the manufacturer installs two (2) insertion marks on the spigots, one for minimum insertion and one for maximum insertion.

The samples display circumferential brittle fractures which are centered on the “crown” or peak of the gasket race.

Some amount of minor erosion was present on the exterior of Sample E1 due to interaction of the escaping water jet and the soil surrounding the joint; this erosion in no way hindered the inspection and understanding of the overall failure mode.

The joints were also found to be slightly deflected with the maximum gap approximately opposite the center of the circumferential fracture length.

The average outside diameters of the spigots and bells were essentially in specification per the AWWA C905-10 requirement (15.300 ± 0.015 inches; 15.285 minimum to 15.315 maximum). Note that a strict determination of conformance to the original specification requirement cannot be made due to the general condition of the samples with slight secondary damage due to installation and removal and surface adhered materials.

Similarly, after removal the gasket dimensions where checked were found to be either in specification or in accordance with expectations for an installed and removed gasket with slightly low thickness and slightly high length dimensions. The hardness of the gasket was also in accordance with expectations, with average results of approximately Shore Durometer A 60.

The gaskets are “Rieber” style with a steel reinforcing ring internal to the gasket and the bell is essentially formed around the gasket during the manufacturing process as follows:

1. The gasket is placed on a fixed outside diameter (OD) mandrel
2. The pipe barrel section where the bell is to be fabricated is heated and expanded over the mandrel and gasket
3. The heated bell area is formed onto the mandrel (typically by vacuum) and cooled forming the bell

The circumferential fractures initiate on the inner wall of the pipe which is “behind” the manufactured-in gasket. The fractures are macroscopically brittle, with little or no ductility in evidence. Figure 4 displays the main fracture area of Sample E1.



Figure 4. Digital image of Sample E1 with circumferential brittle fracture located at the “crown” of the gasket race. Note macroscopically brittle structure, with slight erosion near the center of the fracture.

Circumferential fractures within bell and spigot gasketed PVC piping systems are exceptionally rare. First and foremost, the stress that causes any fracture is oriented perpendicular to the fracture orientation at the origin. As such, the stress which would cause a circumferential fracture would have to be axially (or longitudinally) oriented; because the PVC pipe contains gasketed joints that can move axially, there is essentially no way to develop axial (longitudinal) stresses in the bell from internal pressure. While bending or deflection across the bell/spigot joint can certainly alter the local stress field and generate small axial stresses (as well as shear stresses), these stresses are typically not high enough to cause fracture. Related, if the spigot is over-inserted and the joint is then deflected, the final failure mode is typically an axial fracture initiating at the bell lip. Finally, it should be noted that any failure due to long-term stress, such as that caused by bending, would occur via creep rupture. A creep rupture failure in PVC would display microscopically ductile fracture morphology at the origin of the fracture.

After sectioning open the fracture area of Sample E1 the complete available fracture was inspected visually as well as by optical stereo microscopy. Additionally, a section from near the center (length) of the fracture was inspected using scanning electron microscopy (SEM). Figures 6, 7, and 8 display the fracture morphology at the approximate inner, middle, and outer wall locations at 25X, 150X, and 500X (original) magnification, respectively.

The fracture morphology is microscopically brittle with very little ductility in evidence. In general, fractures in PVC which are both macroscopically brittle as well as microscopically brittle are not common, and typically attributed to environmental stress cracking (ESC) when they occur after installation. High strain rate and/or low temperature effects can also be causative of brittle fractures in PVC but were not considered to be causative in this case since the buried pipeline cannot see low temperatures and once buried cannot be exposed to high strain rate (typically caused by impact events). One typical attribute of ESC failures in general is a multitude of fracture initiations which then coalesce into a larger (single) fracture. Additionally, the fracture origins within ESC failures are typically very brittle, almost “glassy” in appearance, with little microscopic structure in evidence. Note that while some (few) multiple fracture initiations were in evidence along the gasket race crown based on the presence of “steps” in the fracture on the inner wall surface (see Figure 5), no additional initiations were visible anywhere away from the main fracture.

For both samples, while there are certainly more than one fracture origins present within the fractures (based on adjacent fracture “steps” which then join or coalesce into the main fractures; see Figure 5), there were no fracture origins outside of the gasket race crown inner diameter surface. Also, while microscopically brittle, the inner wall fracture structure is not glassy within the fracture surface (see Figures 6-8).



Figure 5. “Steps” present within the Sample E1 fracture. Inside diameter view, with circumferential fracture in the middle of the image running top to bottom. Each “step” represents a distinct fracture origin.

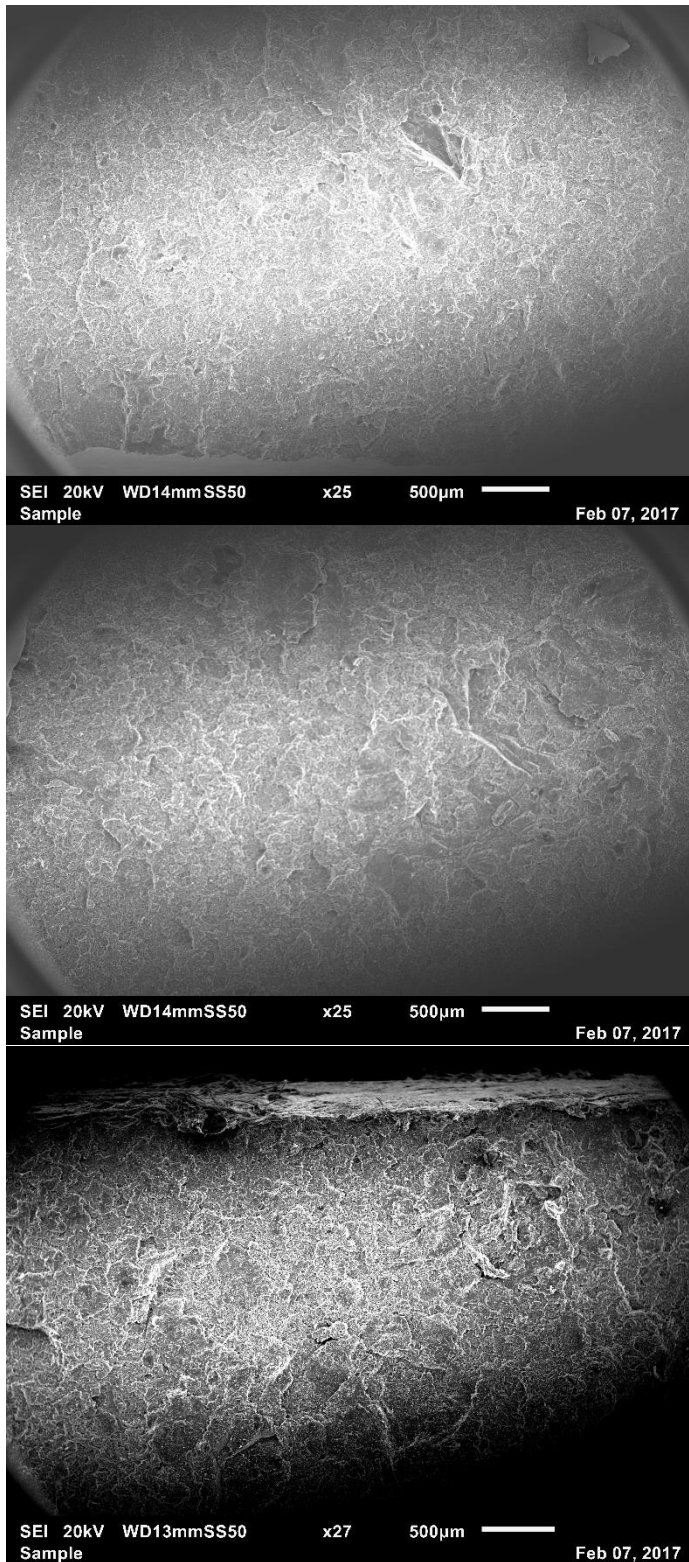


Figure 6. Three SEM images of the Sample E1 fracture at the approximate inner, middle, and outer wall locations (top to bottom respectively; 25X original magnification).

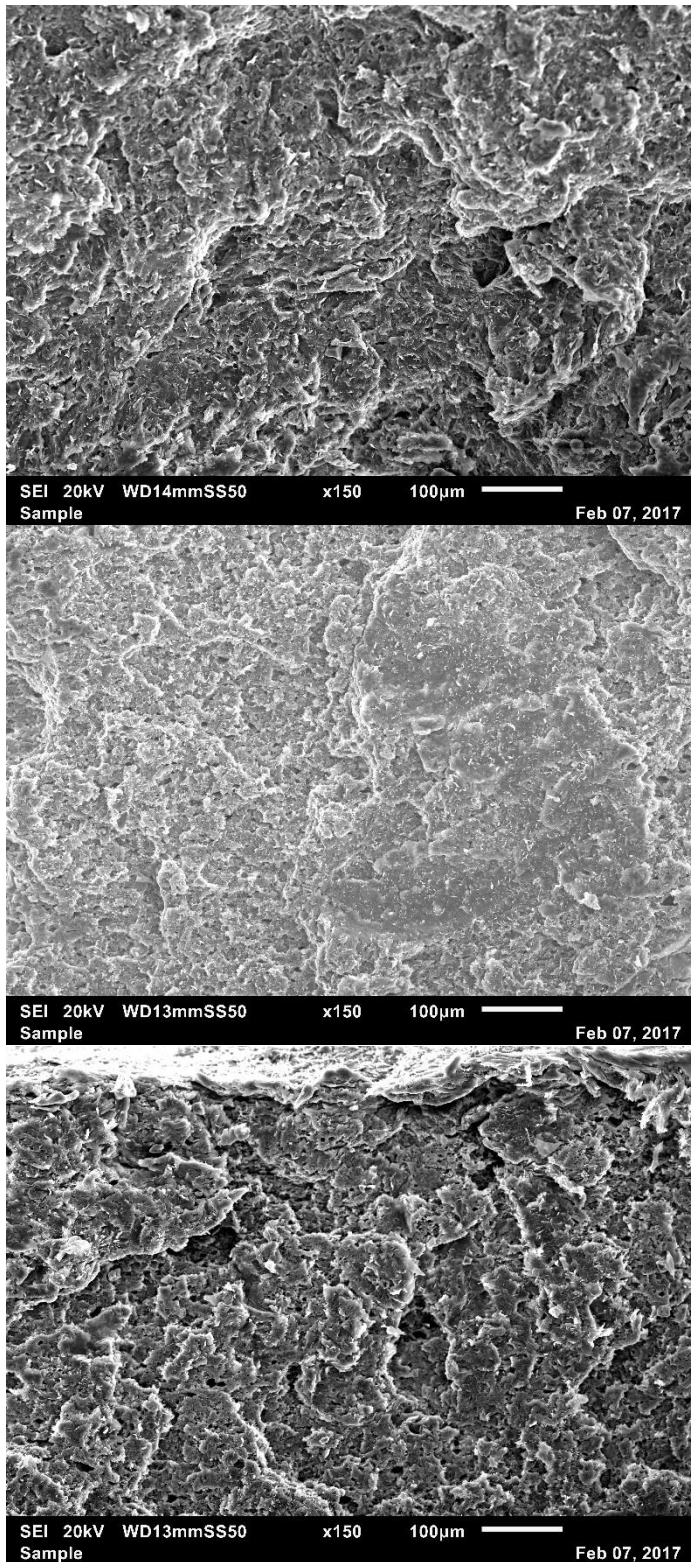


Figure 7. Three SEM images of the Sample E1 fracture at the approximate inner, middle, and outer wall locations (top to bottom respectively: 150X original magnification).

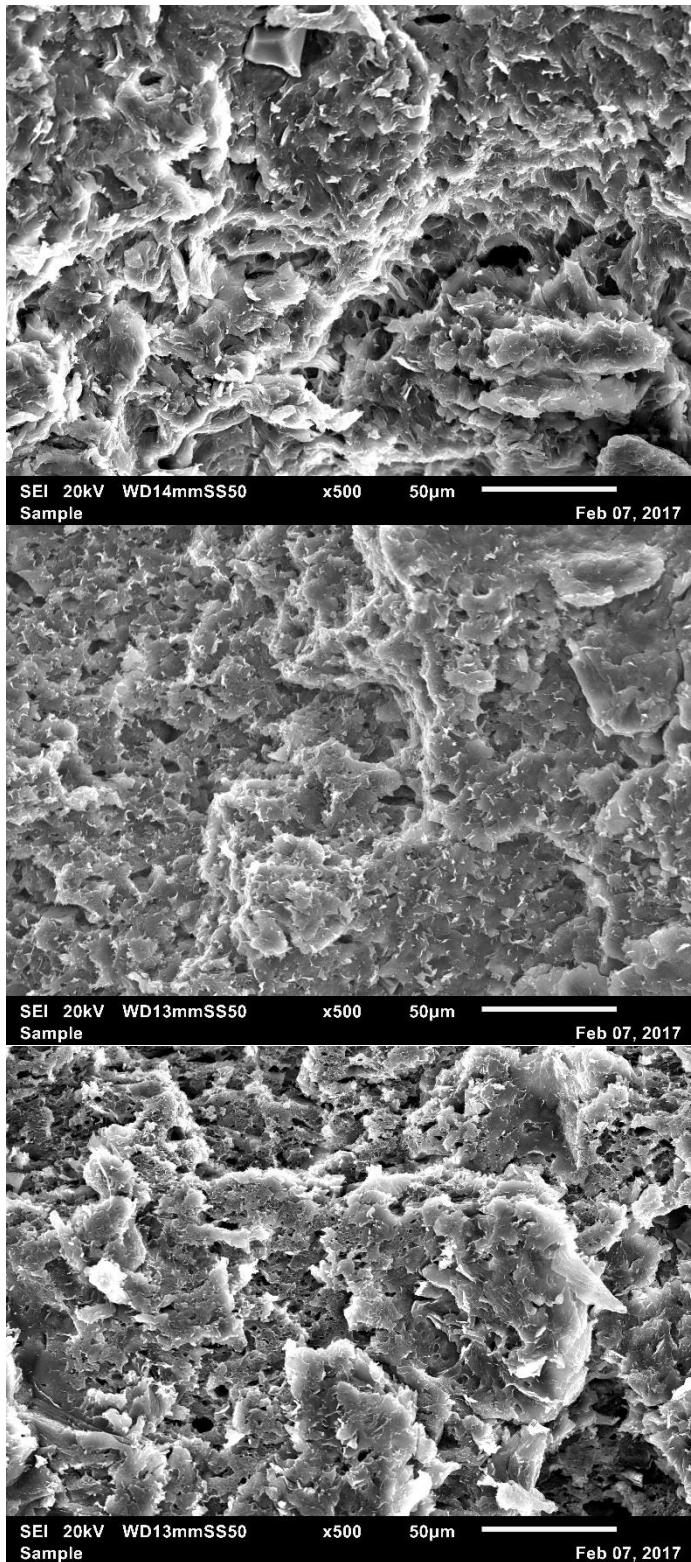


Figure 8. Three SEM images of the Sample E1 fracture at the approximate inner, middle, and outer wall locations (top to bottom respectively: 500X original magnification)

The mechanical properties of the pipe barrel were characterized via tensile testing. Full wall thickness ASTM D638 Type I specimens were tested from Sample E1, as well as reduced wall thickness Type IV specimens with the inner and outer wall surfaces removed. These tensile test specimens were chosen to give an understanding of the mechanical properties of the full wall thickness with any as-found surface condition intact (i.e. incipient ESC fractures and/or other artifacts or conditions), as well as approximate mid-wall material with freshly prepared specimen surfaces. It was hypothesized that the full wall thickness test results would indicate the presence or absence of full scale ESC attack based on comparison of ductility (elongation) to the reduced wall thickness specimens as well as to typical expectations. The samples were generally obtained from two areas within the Sample E1 bell, from near 12 o'clock and from near 6 o'clock. Table 1 below displays the tensile testing results.

Sample	Location	Specimen Type	Tensile Modulus (psi)	Yield Stress (psi)	Strain at Yield (%)	Strain at Break (%)
E1	12 o'clock	I	443,700	6,649	4.47	
			447,900	6,617	4.40	
			438,500	6,666	4.34	
			451,800	6,587	4.21	72
Average			445,500	6,630	4.36	
E1	6 o'clock	I	442,500	6,703	4.43	77
			434,800	6,723	4.44	
			448,900	6,735	4.04	
			Average			442,100
E1	12 o'clock	IV	444,900	6,976	4.00	77
			443,600	6,961	3.98	81
			439,500	6,874	4.15	
			Average			442,700
E1	6 o'clock	IV	441,700	7,026	3.88	78
			441,200	7,018	3.97	
			443,100	6,943	4.10	
			Average			442,000

Table 1. Tensile properties test results from the bell of Sample E1.

The results of the tensile properties testing indicate that the PVC pipe material properties are in general accordance with expectations for an ASTM D1784 12454 material as required within the AWWA C905 product specification material requirements. There also appears to be no evidence of degraded surface condition (e.g. incipient ESC fractures) based on the similar yield and break elongations between the full wall thickness Type I specimens and the reduced wall thickness Type IV specimens.

Regardless of the lack of affected surface condition as determined from the tensile testing results, based on the brittle fracture morphology (both macroscopically as well as microscopically) environmental stress cracking (ESC) was still considered to be a possible root cause. As such, testing was undertaken to search for possible environmental stress cracking agents by FTIR and GC/MS.

Various locations from the samples were tested for the presence of possible environmental stress cracking agents by FTIR as follows:

Residue removed from the gasket race “outside” of the gasket was tested. Figure 9 displays the general location of sampling. Figure 10 displays the stacked FTIR spectra from residue removed from the pressure side of the gasket race as well as the non-pressure side of the gasket race (both on the “outside” surface of the gasket). The spectra are essentially identical and do not display any substantive differences.



Figure 9. Sample E1 gasket race area with circumferential fracture after initial cutting and removal from the bell. Note circumferential fracture at the approximate mid-height of the image (at red arrows), as well as residue present in the gasket race “behind” where the gasket was previously placed. Non-pressure side of the gasket and bell lip are at image top, while the pressure side of the gasket and bell barrel are at image bottom.

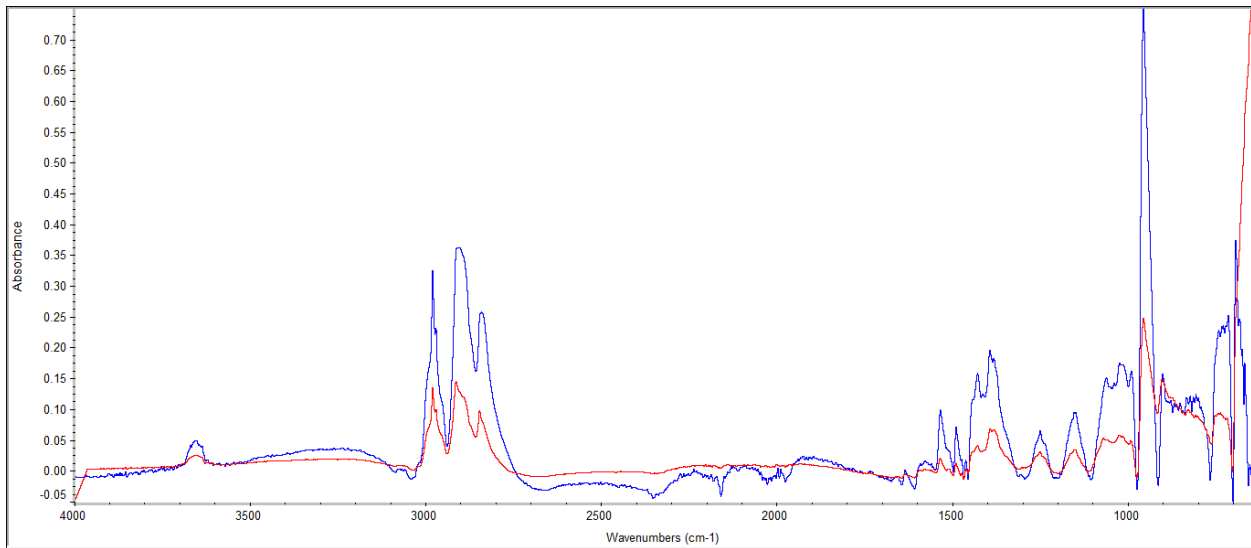


Figure 10. Sample E1 residue sampled from the gasket race (behind the gasket) near the center of the circumferential fracture. Note that these spectra are baseline corrected. The red trace represents the non-pressure (i.e. bell-lip) side of the gasket race while the blue trace represents the pressure (i.e. pipe barrel) side of the gasket race. Note also the generally similar if not practically identical chemical makeup based on the presence of identical peaks within each spectrum.

Three different locations from the pipe inside diameter surface within the (pressure side) bell barrel area were removed from Sample E1 and tested. Figure 11 displays the stacked FTIR spectra from these locations. The spectra are generally similar and do not display any substantive differences.

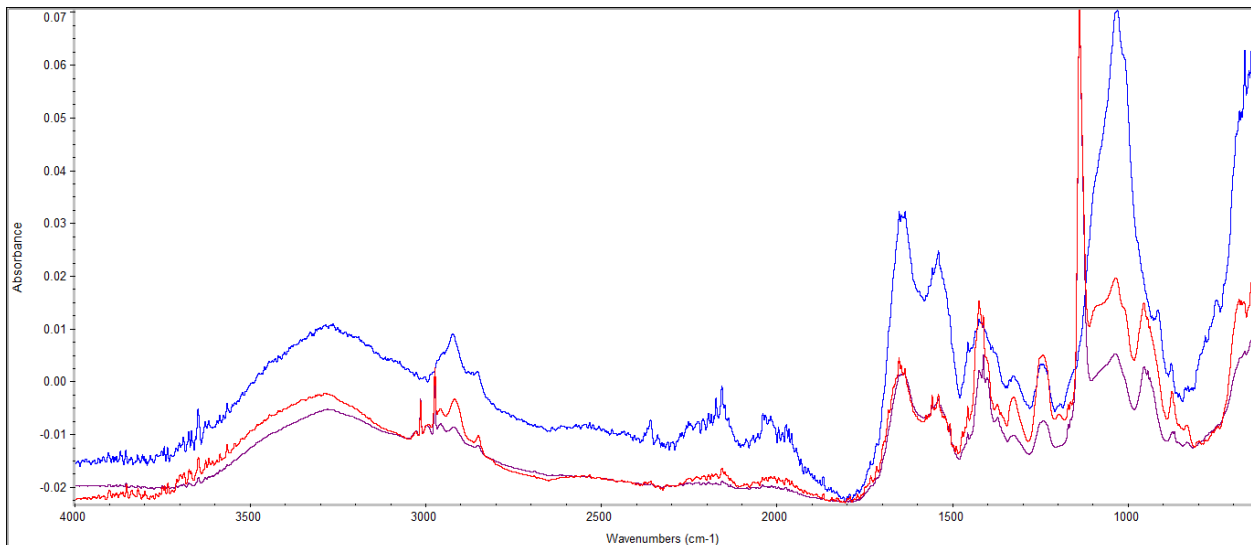


Figure 11. Sample E1 joint residue sampled from the (pressure side) bell barrel ID surface. Note the generally similar chemical makeup based on the presence of identical peaks within each spectrum.

Two different locations from the pipe inside diameter surface within the bell barrel area were removed from Sample E2 and tested. Figure 12 displays the FTIR spectrum from the (non-pressure side) spigot lip location. Figure 13 displays the FTIR spectrum from the (pressure side) bell barrel location. The spectrum in Figure 13 is generally similar to the spectra from Sample E1 obtained from similar locations (see also Figure 11 above for comparison to the Sample E1 results).

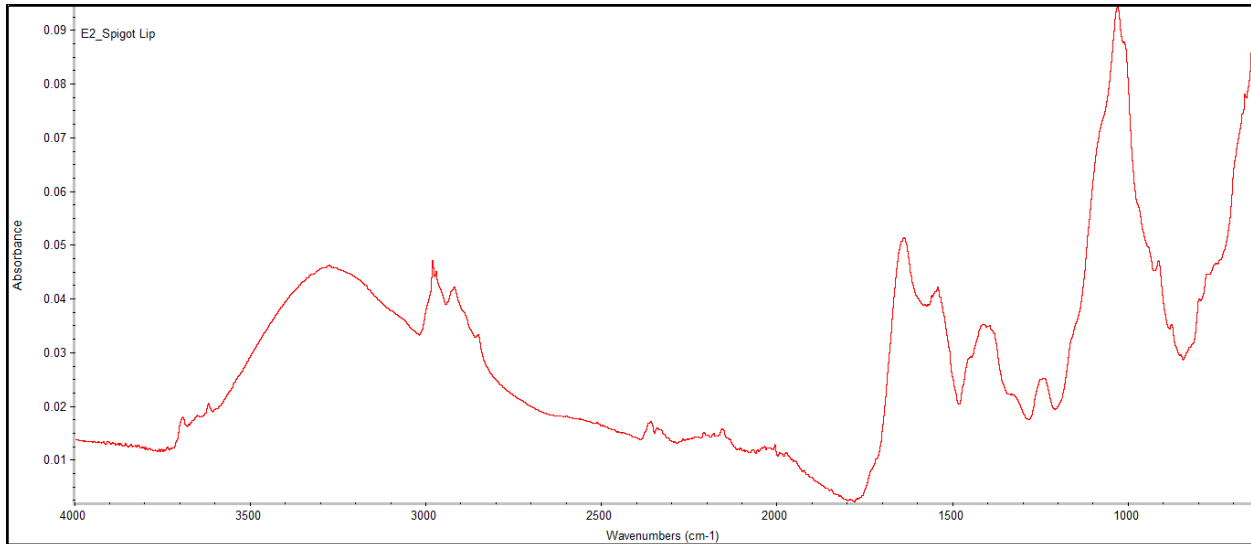


Figure 12. Sample E2 joint residue sampled from the bell ID at the (pressure side) bell lip.

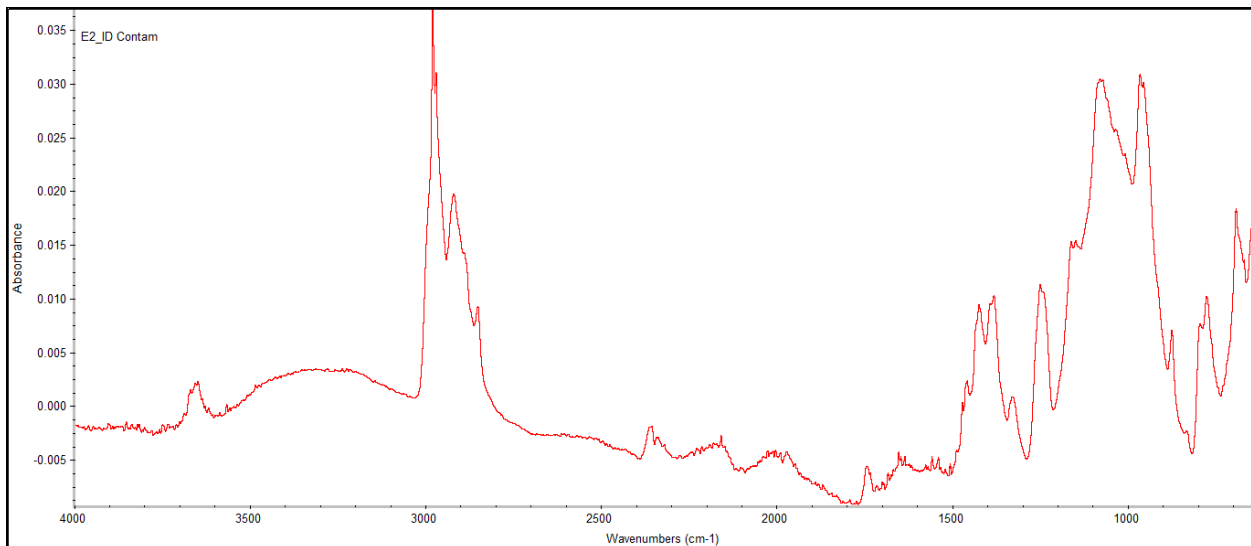


Figure 13. Sample E2 joint residue sampled from the (pressure side) bell barrel ID. Note the generally similar chemical makeup to the similar sampling locations from Sample E1 based on the presence of identical peaks within each spectrum (see also Figure 13).

Interpreting the complete body of inner wall residue FTIR test results, the inner wall residue was determined to be a mixture of multiple materials with similar but slightly different chemistries. Some of the possible chemistries present within the inner wall contamination were esters, surfactants, possibly ethers, and possibly formaldehyde. Due to the fact that the inner wall residue was an inhomogeneous mixture of materials, definitive identification via FTIR was not possible without significant additional sample preparation (i.e. separatory) steps.

One section from near the center of the Sample E1 fracture was sent for GC/MS testing where the fracture surface as well as the inner wall (including the fracture surface) were solvent washed with ethanol and hexane. Both Sample E1 and Sample E2 were tested in nearly identical manner. The fracture surface (only) rinsates yielded very little information, most likely due to the small areas involved as well as the lack of volatility/solubility of the compounds within the residue. The hexane rinsate of the Sample E1 inner wall (and fracture surface) indicated the presence of phthalates and esters in low (estimated) concentrations, as well as alkanes (waxes). The ethanol rinsate of the Sample E1 inner wall (and fracture surface) indicated the presence of acrylates, phthalates, adipates in low (estimated) concentrations, as well as phenolics and alkanes (waxes). The Sample E2 rinsates were similar to the Sample E1 rinsates, although with comparatively lower yields and compound identifications.

Interpreting the complete body of GC/MS data from inner wall rinsates, the phthalates and esters, and possibly the adipates and phenolics, could be potential environmental stress cracking agents for PVC materials.

The gasket material from the Sample E1 gasket was tested using GC/MS via Heated Headspace sample introduction. An approximately 1 gram sample was heated to a maximum temperature of 180°C during testing. Only a few compounds were detected, and the most likely source of these compounds is presumed to be the rubber material and/or additive package(s) although some additional analytical effort would be needed to fully understand these results.

The elastomeric (rubber) material of the gasket was determined via pyrolysis FTIR. A small sample of the Sample E2 gasket was pyrolyzed and the condensate was then analyzed by FTIR. The gasket material was identified as a styrene butadiene rubber (SBR) material. Figure 14 displays the pyrolysis FTIR test results from the pressure and non-pressure sides of the Sample E2 gasket. Figure 15 displays the pyrolysis FTIR test results from the pressure side of the Sample E2 gasket stacked with a new exemplar gasket sample prepared in identical fashion. Figure 16 displays the new exemplar gasket sample pyrolysis FTIR spectrum matched to a library reference spectrum for styrene butadiene rubber (SBR).

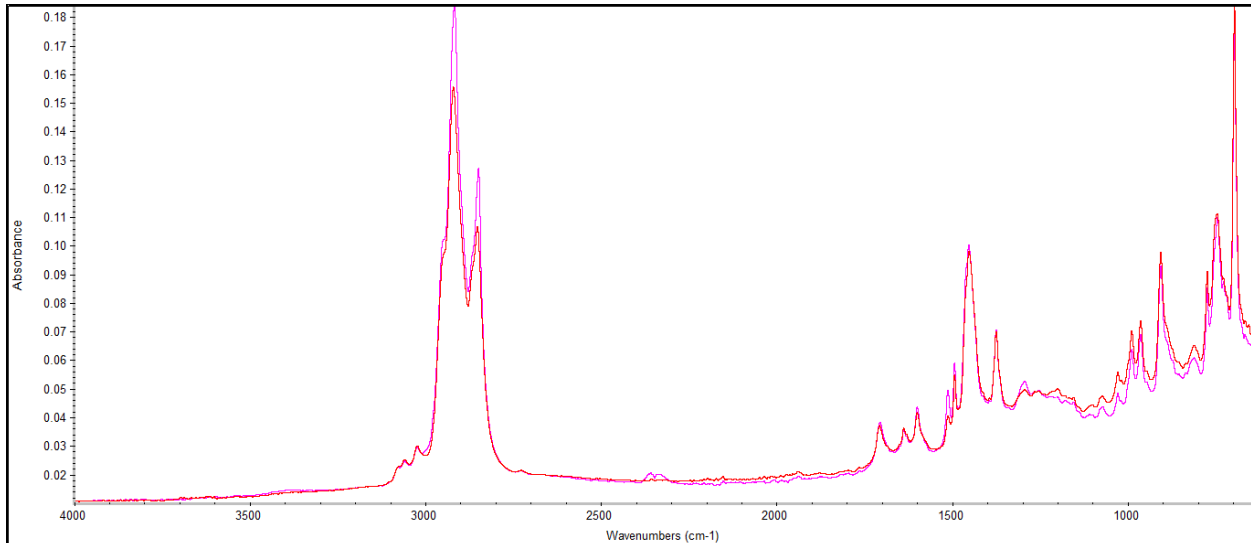


Figure 14. Sample E2 gasket pyrolysis FTIR test results from the pressure and non-pressure sides of the gasket. Note the identical chemical makeup based on the presence of identical peaks within each spectrum.

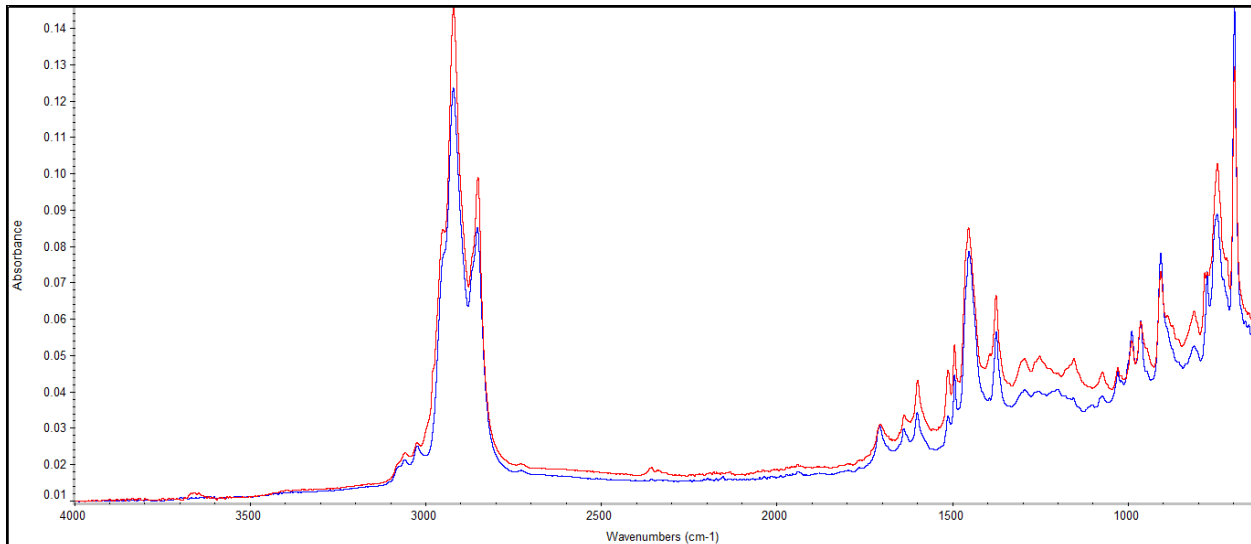


Figure 15. Sample E2 gasket pyrolysis FTIR test results from the pressure side of the gasket stacked with the pyrolysis FTIR spectrum of the new exemplar gasket sample prepared in identical fashion. Note the identical chemical makeup based on the presence of identical peaks within each spectrum.

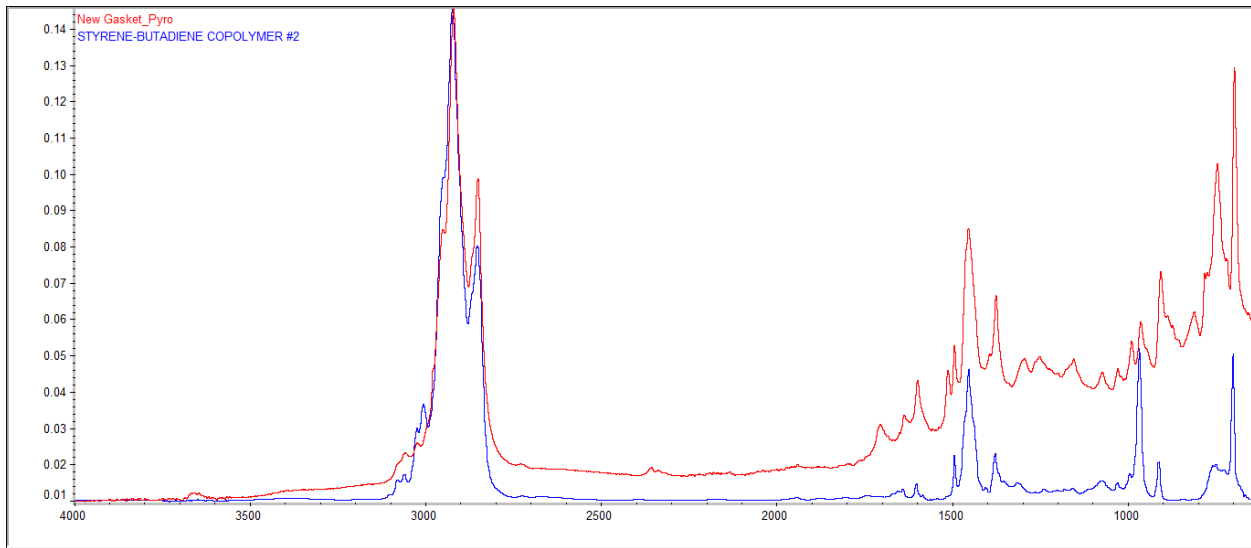


Figure 16. New exemplar gasket sample pyrolysis FTIR spectrum matched to a library reference spectrum for styrene butadiene rubber (SBR).

Interpreting the complete body of gasket pyrolysis FTIR test results, the gasket material from Sample E2 was identical on the pressure and non-pressure sides of the gasket. The Sample E2 gasket material was also identical to a new exemplar gasket material provided by the pipe manufacturer. The Sample E2 gasket is identified as an SBR material, which was later confirmed via discussion with the gasket manufacturer.

Regarding the joint assembly workmanship and alignment, the two samples were received in generally straight alignment, although some deflection was evident based upon annular gaps around the bell lip circumference. As noted prior, the spigots were appropriately belled, i.e. generally inserted to the manufacturer's recommended minimum insertion mark, i.e. just up to the first of the two manufacturer's marks. There was some amount of fine-grained debris in the joint area, both in the gap between the gasket sealing lobes as well as fore and aft of the gasket, including behind the gasket as previously discussed, with Sample E2 containing much more of this fine grained debris in comparison (see Figure 17). Note that the fine grained debris was most likely NOT present during insertion as no translational artifacts were noted within the debris filled areas.



Figure 17. Sample E2 just after extraction of the spigot and gasket by sectioning and disassembly. Note fine grained debris present on both sides of the gasket race. Also note circumferential fracture at the gasket race at the as-installed 12 o'clock location (near image bottom with small section missing).

Sample E2 was further sectioned to provide approximately 1 inch wide strips from the 3, 6, and 9 o'clock locations which were used as a gross ductility check for the material specifically within the gasket race (also in comparison to the tensile properties test results discussed above). These strips were secured in a vise at the bell lip, then bent approximately 90-120 degrees back on itself, typically described as a “bendback” test, placing the inner wall at the crown of the gasket race in tension (see Figure 18). Two of the three bendback test samples fractured, although the microscopic fracture morphology at origin at the inner diameter surface at the top of the gasket race was ductile; there were no pre-existing fractures in evidence. Bendback test samples from the 6 and 9 o'clock locations fractured, while the 3 o'clock location did not.

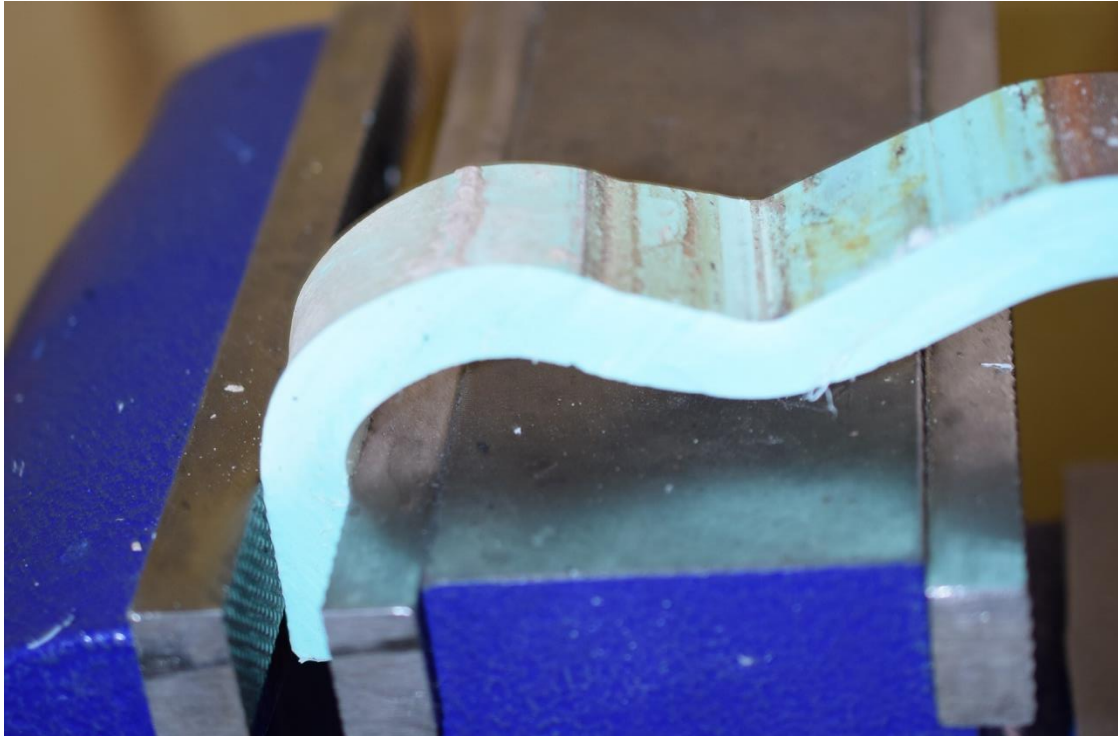


Figure 18. Typical Sample E2 gasket race ductility check by bendback testing. Note ability to deflect at the bell lip with gross ductility in evidence (Sample E2, 3 o'clock test sample specifically).

CONCLUSIONS, OPINIONS, AND DISCUSSIONS

In general, the microscopically and macroscopically brittle fracture mechanism (which took some unknown amount of time after installation to develop) can only typically be caused by environmental stress cracking (ESC). However, as discussed extensively above, the evidence in hand does not fully support ESC as the primary cause of failure, mainly due to the lack of incipient microcracking outside of the crown of the gasket race and retained ductility displayed within the tensile and bend back testing, even though the GC/MS testing indicates the presence of potential chemical stress cracking agents. Related to this, the circumferential orientation of the fractures is atypical of ESC (and almost all other) failure modes.

It should be noted that no manufacturing defects or workmanship defects could be causative of the brittle fractures in evidence.

Since the fractures are oriented in the circumferential direction, this is empirical evidence that the peak stress field was (locally at fracture origin) in the axial or longitudinal direction; note that the principal stress from operation is oriented in the hoop direction due to pressurization. As such it is hypothesized that the failures investigated herein were caused by swelling of the gaskets by some yet to be fully explained process which placed the bell areas of the PVC pipe in triaxial stress or plane strain condition which caused the brittle fracture. The triaxial stress state exists when a component is simultaneously stressed along all three principal (x, y, and z) axes. When this occurs the material is hindered from necking, drawing, or otherwise responding in a ductile manner. The fracture morphology resulting from triaxial stress would be expected to be microscopically and macroscopically brittle.

Ample evidence exists to support this gasket swelling hypothesis. The macroscopic fracture network is oriented in the circumferential direction and present only in the crown of the gasket race. Since bell and spigot PVC pipe sections can move translationally at the gasket interface, no significant stresses can be imparted to the wall of the bell by any outside force, deflection, etc. The stress therefore has to come from the gasket itself, and since the gasket is typically an inert solid in water service the gasket had to be altered in some manner. Swelling of SBR and other sealing materials due to solvents is a common industrial problem and is most likely the root cause of the circumferential bell fractures investigated herein. While extensive chemical analysis testing was performed (e.g. FTIR, GC/MS, and Heated Headspace GC/MS), no chemistries that would result in gross swelling of the gaskets were detected. This is almost certainly due to the age of the line and the time that it had sat stagnant (from fall of 2016) and/or the time which the samples had been open and exposed to air after removal. However, research of test results for compounds reported by Great Lakes Chemical Corporation (GLCC) to the regulatory agencies as present in process wastewaters and/or manufacturing processes within the GLCC site, from which the treated water is pumped into the pipeline, indicates that brominated chemicals as well as acetone, methylene chloride, and methanol would all be present in wastewaters not discharged into the Ouachita Joint Pipeline but disposed via underground injection. The acetone and methylene chloride would certainly be detrimental to the SBR gasket material and cause swelling, as well as the other compounds present within the GLCC process solutions. As such it is hypothesized that a discharge into the pipeline of water containing these volatile chemical solvents occurred prior to the failures. While the exact timing and course of events which led to this discharge and subsequent failures are not yet known, the phenolic compounds within the bell inner wall surface rinsate sample GC/MS test results are indicative of this (and of low enough volatility to still be detected). Conversely, the acetone, methylene chloride, and methanol are highly volatile thus explaining our inability to detect the source of the chemical which caused swelling of the gaskets. Also supporting this hypothesized failure mode, the client reported that significant lengths of 14-inch bell and spigot gasketed PVC pipe manufactured by JM Eagle at approximately the same time (March 2012), and installed at approximately the same time (2013), have not experienced any failures to date.

During the March 2017 El Dorado, AR site visit by S. Ferry where various additional joints were excavated a second joint failure mode was discovered, specifically leakage without fracture (4 of 17 total failures). While still present at the pipeline one of these leaking joints was disassembled in the field. The joint appeared to have been appropriately assembled (up to the manufacturer's minimum insertion mark) and there was no evidence of poor workmanship. The gasket was still retained within the gasket race and had no evidence of "rolls" or tears which would be typical of a leaking gasket. Similar to Samples E1 and E2, there was some amount of fine grained debris present in the joint area, which appeared to have been introduced AFTER assembly of the joint, again because of the presence of this material "behind" the gasket within the gasket race area and lack of translational damage artifacts which are typical of "dirty" installations (see Figure 19).

The mode of failure in all cases, both circumferential bell fracture as well as leaking joints, is hypothesized to have occurred as follows:

1. Exposure of the gaskets to solvents
2. Swelling of the gaskets due to solvent interaction
 - a. Achievement of strain sufficient to fracture the bell via triaxial stress state (for the circumferential bell fracture population)
 - b. Accommodation of the swollen gasket without fracture (for the leaking gasket population)
3. Reduction of gaskets upon removal of solvent
 - a. Gross leakage through now-fractured bell
 - b. Leakage through compromised gasket race area with debris present

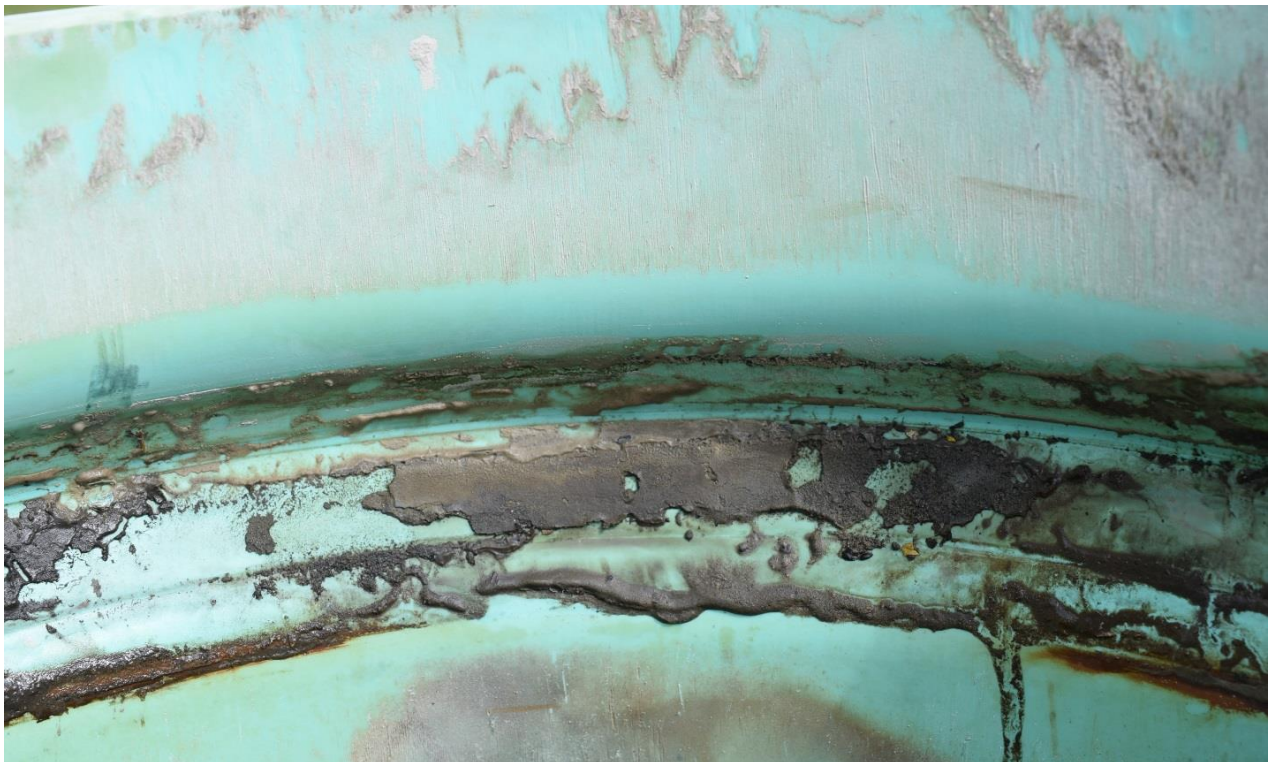



Figure 19. Sample E10 just after extraction of the spigot and gasket in the field. Note fine grained debris predominantly present on the pressure side of gasket race. Bell lip is at image top.

Following the site visit by S. Ferry the pipeline was reportedly repaired sufficient to allow for a pressure test. While no definitive statements can be made, the pressure test result should be sufficient to establish that no through-wall circumferential bell fractures exist in the pipeline in its current condition. However, the possibility exists that leaking (i.e. non-fracture) failures could still exist, and/or incipient circumferential bell fractures could exist in the 14-inch GLCC pipeline such that future failures may still occur based on the prior exposure to chemical compounds which compromised the gaskets and sealing integrity of the joints. Based on the failure locations within the 14-inch GLCC pipeline, i.e. within the first 5350 feet of the approximately 12,500 foot pipeline (or 43% of the linear distance), future failures, if they occur, would be expected to occur within the same general locations. Related, since no failures have occurred within the downstream combined flow 30-inch line sections (which have remained operational) this portion of the pipeline is surmised to have not been similarly affected as the upstream section which has exhibited significant failures (6.3% joint failure rate within the 5350 length).

Additional extensive testing may be performed on samples removed and/or obtained during the March site visit. This includes a selection of the tests described within this report, as well as some amount of additional testing. Items proposed for additional future testing include failure analysis of both leaking and circumferential bell fractures, product specification testing of never-installed joint samples left over from the original installation, testing of never-installed pipe in an attempt to duplicate the field failure mode (via purposeful introduction of solvents into a sustained pressure test sample), and possibly finite element analysis of the joint envelope modeling stresses induced by gasket swelling as well as other yet to be developed methods.

Two items are attached at the end of this report: Figure 20 displays a client-provided view of the first approximately 5400 feet of the pipeline with failure locations and pipeline elevations marked thereon. Table 2 displays a rollup of information pertinent to the failure population.

Report Written by:



Steve Ferry
Laboratory Director

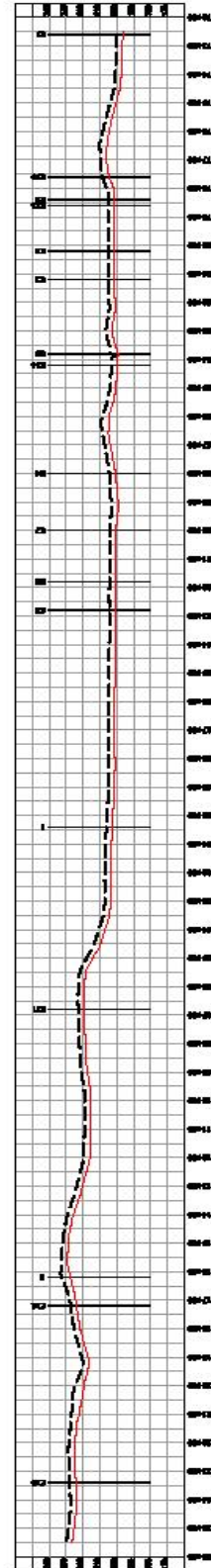
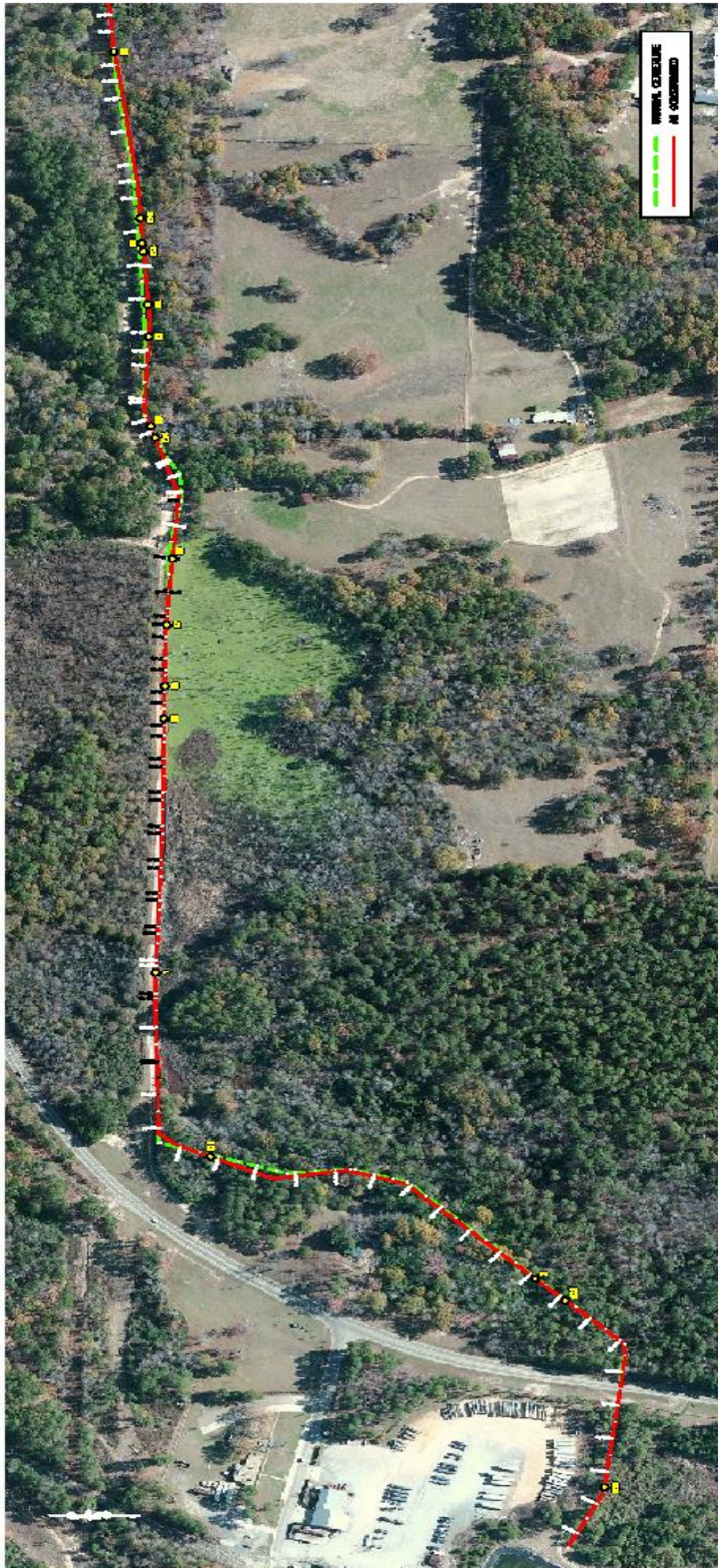


Figure 20.

Failure Identification	Discovery Date	Repair Date	Failure Mode	Approximate Location	Pipe Printline Date Code
1	10/27/2016	10/27/2016	CBF	100+40	2012/MAR/26
2	11/8/2016	11/9/2016	CBF	116+20	2012/MAR/26
E1	11/9/2016	11/17/2016	CBF	72+60	2012/MAR/25 and 2012/MAR/27
E2	11/9/2016	11/15/2016	CBF	80+20	2012/MAR/24 and 2012/MAR/25
E3	11/9/2016	11/16/2016	CBF	81+20	
E4	11/9/2016	3/15/2017	CBF	88+00	2012/MAR/25
E5	11/9/2016	3/20/2017	CBF	92+80	
E6	11/17/2016	3/15/2017	Leakage	83+80	2012/MAR/24
E7	3/13/2017	3/14/2017	CBF	90+00	2012/MAR/25
E8	3/13/2017	3/20/2017	Leakage	91+80	
E9	3/14/2017	3/16/2017	Leakage	78+40	2012/MAR/25
E10	3/14/2017	3/16/2017	Leakage	77+60	
E11	3/15/2017	3/17/2017	CBF	106+80	
E12	3/21/2017	3/22/2017	CBF	117+20	
E13	3/21/2017	3/22/2017	CBF	78+60	
E14	4/4/2017	4/4/2017	CBF	84+20	
E15	4/4/2017	4/5/2017	CBF	123+40	

Table 2. Tabulated rollup of information pertinent to the failure population known as of the date of this report. “CBF” denotes circumferential bell fracture failure mode. “Leakage” denotes bell/spigot joint leakage failure mode without fracture.